

Extensive Air Showers Near the Knee

J. Matthews^{a,b}

(a) *Dept. of Physics and Astronomy, Louisiana State University, Baton Rouge, LA 70803 USA*

(b) *Dept. of Physics, Southern University, Baton Rouge, LA 70813 USA*

Presenter: James Matthews (matthews@phys.lsu.edu)

We summarize new and important results given at the 29th International Cosmic Ray Conference on experimental measurements and simulations of extensive air showers near the knee of the spectrum. Most results on the shape of the spectrum and the composition are consistent with Fermi acceleration in SNR. The newest versions of hadronic models in simulations are providing more similar predictions of air shower structure, but some notable problems remain.

1. Introduction

The most intriguing feature of the energy spectrum of cosmic rays is that its form is a power law, the flux diminishing with energy as $E^{-\gamma}$. The spectral index γ of the differential flux has been observed to maintain a constant value of about 2.7 until a few PeV, then changes to about 3.1 for at least three more decades in energy. Such a non-thermal spectrum strongly suggests that it arises from interesting, very energetic processes whose nature is not yet known. The change in the index is known as the “knee” in the spectrum.

The most popular explanation of this behavior is that primary cosmic ray particles are accelerated in the plasma shock waves from Galactic supernovae. This process, called Fermi Acceleration, naturally produces a power law spectrum with a spectral index of nearly the observed value. Moreover, the predicted value of the spectral index is largely insensitive to the details of the progenitor SN, as long as the shock is “strong”. The difficulty with this model is that the maximum energies attainable are limited by the useful lifetime of the shock, with most calculations yielding E_{\max} near, but less than, 1 PeV. While such an energetic limit is surely near enough to the “knee” to give much credibility to the hypothesis, there is no ready explanation for the continuance of the spectrum as a power law beyond this point with only slightly steeper behavior.

At this conference, direct evidence was presented for the first time for the acceleration of cosmic rays via the Fermi mechanism in the expanding shells of Galactic supernovae. The HESS experiment imaged TeV gamma rays from the outer edges of SNR [1]. These gamma rays are presumed to come from interactions of higher energy charged primary particles undergoing Fermi acceleration.

Beyond TeV energies, direct measurement of cosmic rays is not practical, due to the low flux. Instead, indirect study via the measurement of extensive air showers in the atmosphere is required. Confirmation of the Fermi acceleration hypothesis would rest on two observational pillars: (1) the steepening of the energy spectrum at the knee should be relatively smooth, otherwise one may be observing some new acceleration process overtaking the one which operates at lower energy, and (2) the composition of charged primary cosmic rays should become heavier through the knee region, since E_{\max} is proportional to the charge of the primary (as would be true for any electromagnetic acceleration process).

This review will summarize some of the presentations which addressed questions relating to the spectrum, composition, and nature of cosmic rays near the “knee” in the spectrum. This work is drawn from some, but not all, of the many contributions in sessions HE 1.1, HE 1.2, HE 1.5, and HE 2.1.

2. New and Recent Projects

We begin by outlining some of the newer projects which reported results at the conference.

The ARGO-YBJ experiment is currently under construction at the Yangbajing Cosmic Ray Laboratory in Tibet [2]. This project employs a densely packed, “full coverage” array of resistive-plate chambers at high altitude (4300 meters above sea-level, m.a.s.l.) to study cosmic rays at a low threshold, about 100 GeV, through the knee region. A thin lead-converter layer is above the detectors to give extra sensitivity to photons in air showers, allowing detailed study of the shower front structure. Presently, 3500 m² of active area (out of total planned area of 6500 m²) have been instrumented. First results were given for 1900 m² of detectors which have been taking data since December 2004.

Results on searches for 100 TeV events from the direction of EGRET gamma-ray sources were presented by a group from Teheran, Iran, using a small scintillator array [3]. No unusual deviations from normal fluctuations were observed (see Figure 1); upper limits on ten such sources were given. The group plans to enlarge this experiment and run it in the ALBORZ observatory in Teheran.

On Mt. Aragats, Armenia, the GAMMA installation [4] is a ground based array of 33 surface particle detection stations and 150 underground muon detectors at an elevation of 3200 m.a.s.l. (700 g/cm²). The surface stations of the EAS array are located on 5 concentric circles of radii 20, 28, 50, 70, 100m. Each station contains 3 square plastic scintillators, each 1x1x0.05m. The underground muon detectors (the “muon carpet”) are compactly arranged in an underground hall under 2.3 kg/cm² of rock.

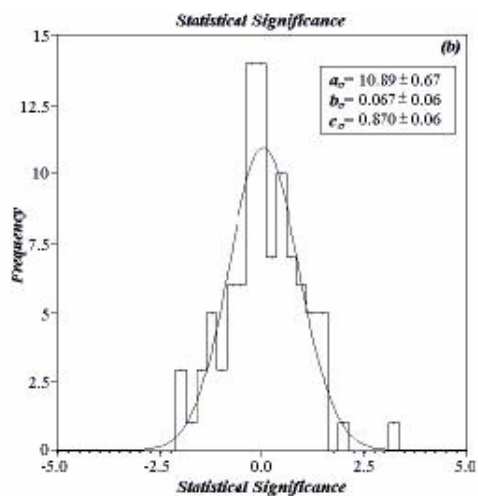


Figure 1. Results from the Teheran array on the significance of excesses from the direction of EGRET sources.

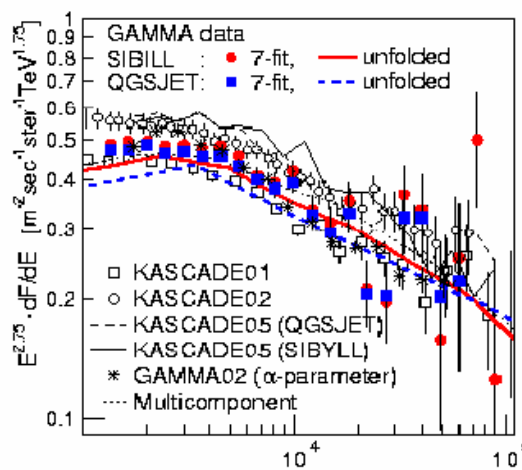


Figure 2. Flux vs. energy (TeV) from GAMMA experiment

The good muon coverage allows multidimensional analysis of air showers for determining primary energy and composition. The group uses such an unfolding algorithm with two different simulations. Figure 2 shows the all-particle energy spectrum from the GAMMA array calculated using these two air shower hadronic-interaction simulation codes, SIBYLL and QGSJET.

3. Experimental Results

Several long-running experiments presented new results at the conference. We review a selection of these, with special emphasis on the most extensive projects, the KASCADE and EAS-TOP experiments.

The Tunka experiment [5] uses an array of 25 wide angle photodetectors to measure the lateral distribution (LDF) of Cherenkov light. The purpose is to establish the depth in the atmosphere of maximum shower development, X_{\max} which is sensitive to the composition. Results of a new analysis of their experimental data were given. Two different methods to estimate X_{\max} were used: one based on the pulse width, another on the shape of the LDF. A new function to fit the Cherenkov light lateral distribution LDF at core distances from 0 to 350 m has been developed using CORSIKA simulations, and two versions of the QGSJET interaction simulator. The results are given in Figure 3. The composition shows a tendency to become heavier at about 10^{16} eV, although the proportions of heavy and light primaries depends on the simulation. (We discuss more fully the two QGSJET versions later, in section 4 below).

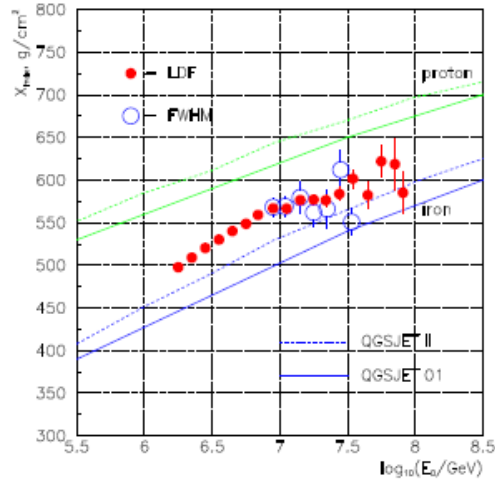


Figure 3: Depth of shower maximum, from TUNKA-25.

GRAPES-3 is a high-density air shower array with large area muon detectors[6]. The energy spectra of various nuclei (H, He, N, Al and Fe) and their mean mass have been obtained through a combination of observations on electrons and muons. The mean mass number gradually increases through the knee region. These results show dependence on the hadronic interaction models of EAS Monte Carlo. Two models, QGSJET and SIBYLL, were investigated and their results were compared with those from direct measurements. Predictions of SIBYLL agree with JACEE results, but some discrepancy is seen between QGSJET and JACEE. The group discussed their results in terms of several models proposed in literature.

We turn here to the long-running KASCADE and EAS-TOP experiments that both presented extensive analyses of both the energy spectrum and the composition of cosmic rays near the knee. We summarize here the main results from both projects.

The EAS-TOP array analyzes its data through simultaneous measurements of the electromagnetic and muon components of extensive air showers[7]. The array is located at Campo Imperatore, 2005 m.a.s.l. ($820/\text{cm}^2$) at the National Gran Sasso Laboratories, on the mountaintop above the underground laboratory halls there.

The main components of EAS-TOP include a surface array with target area $A = 10^5 \text{ m}^2$ and sensitive area 330 m^2 , as well as 140 m^2 of tracking muon detectors. The latter system has a muon energy threshold about 1 GeV . The array also has operated in coincidence with two underground detectors, the LVD and the MACRO experiments. This combination permits study of air shower muons with energies above 1.3 TeV at the top of the mountain.

Data are interpreted using simulations with two different interaction models (QGSJET and SYBILL) inside the CORSIKA shower simulation framework[8]. The data are “unfolded” in comparison to simulation predictions to obtain the most likely combinations of primary particle type and spectra. Proton and helium (“p+He”) and proton, helium and CNO (“p+He+CNO”) groupings of primaries are selected at $E > 80 \text{ TeV}$, and at $E > 250 \text{ TeV}$ respectively. Results using GeV and TeV muons are shown in Figure 4. The knee is visible in the all-particle spectrum at about 5 PeV , and the composition exhibits a tendency toward heavier primaries.

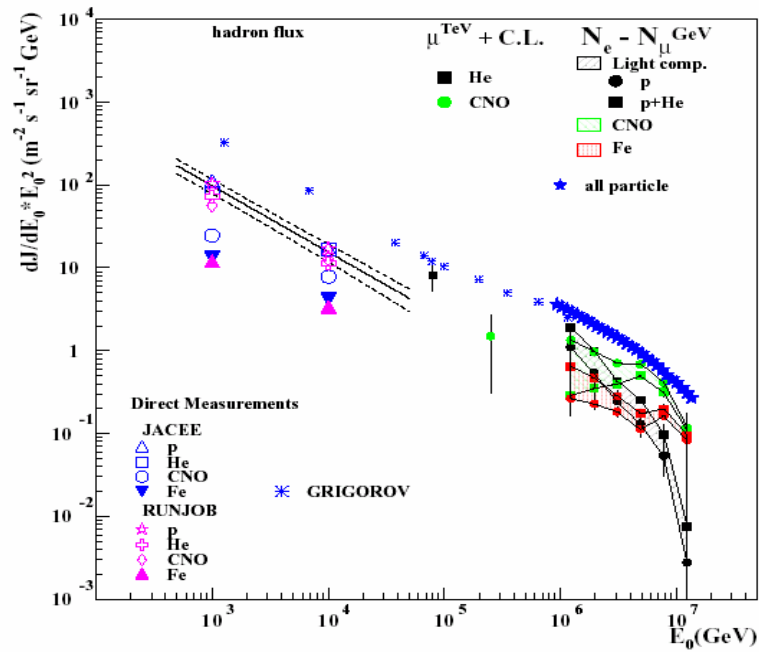


Figure 4: Summary of energy spectra measurements from EASTOP, using both underground (TeV) muons and surface (GeV) muon measurements. Some direct measurements are shown for comparison.

Figure 5 shows a closer look at this trend, the grouping of data into just two components, “heavy” and “light”, as interpreted using the TeV muon data. The energy spectrum of “light” primaries is beginning to diminish at about $5 \times 10^{15} \text{ eV}$, whilst the “heavy” component spectrum may be signaling its change at least a decade higher in energy. The trend toward generally heavier composition is evident both in analyses with the

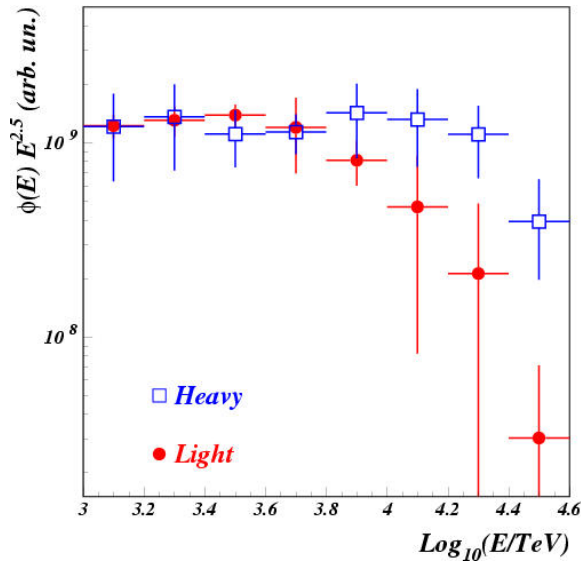


Figure 5. EASTOP with MACRO results using TeV muons.

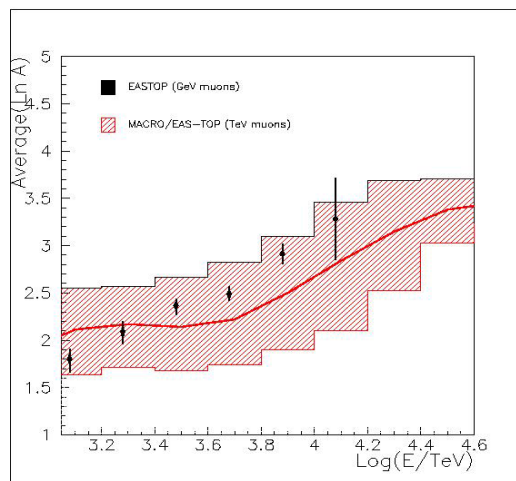


Figure 6. Comparison of composition results from EASTOP using GeV and TeV muons.

GeV muons and with the TeV muons, but there is a systematic difference in absolute proportions between the two studies (Figure 6). The cause is unclear, but suggestive of some difficulty with the simulations, either in the interaction models or in the transport of the muons through the rock from EAS-TOP to MACRO.

The KASCADE experiment[9] reported extensively on analyses of the cosmic ray spectrum and composition. This project is located near sea-level in Karlsruhe, Germany, and has detectors for measurement of the electromagnetic, muonic, and hadronic components of air showers. This experiment has been operating and enlarging for over a decade. There are several major components of the project allowing study of the properties of air showers from 10^{14} eV to nearly 10^{18} eV. Of particular note are several separate muon detection systems permitting simultaneous measurement of muons with four different energy thresholds.

The basic KASCADE surface array extends over 200m x 200m with 252 detector stations arranged on a rectangular grid with 13 meter spacing. Each station has four detectors for electrons and photons, as well as one for muons above 250 MeV (using a iron-lead-absorber of about 20 attenuation lengths). The effective detection area per station is about 3.2m^2 for both detector types. In addition to the surface array, there is a muon tracking detector using limited streamer tubes, measuring muons above 800 MeV. In the center of the array, there is a collection of detectors including a hadron calorimeter and two shielded muon detectors with thresholds of 490 MeV and 2.4 GeV. Muon densities are reconstructed for radial distances up to 700 m.

The KASCADE systems have now been surrounded with a larger array, GRANDE, which was built by reassembling 37 stations of the former EAS-TOP experiment[10,11]. The KASCADE-Grande stations are spaced about 130 m covering an area of 0.5 km^2 next to the KASCADE site in order to operate jointly with the KASCADE detector components. Each KASCADE-Grande array station is equipped with 10 m^2 of scintillation counters and the electronic components to generate a trigger signal and for calibration purposes. A central data acquisition station (DAQ) collects the data from all stations and generates a valid experiment trigger. KASCADE and the Grande array have taken data in coincidence since December 2002 and allow a multiparameter measurement of extensive air showers up to about 10^{18} eV

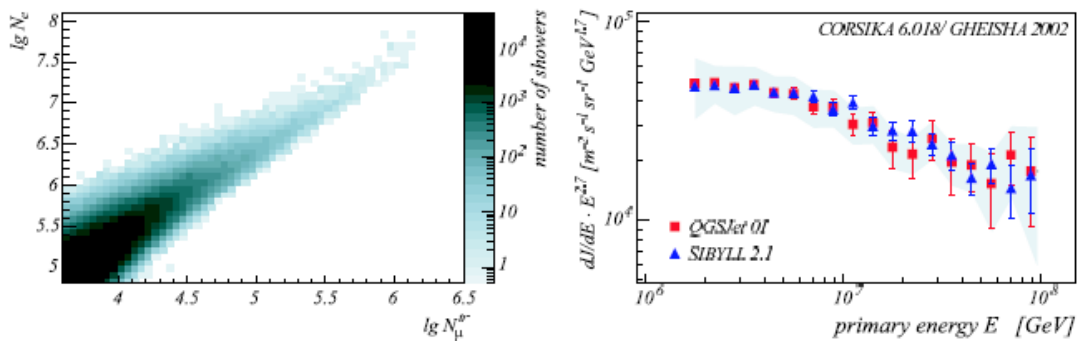


Figure 7: Left: Two-dimensional shower size spectrum as measured by KASCADE. Right: Result for the all particle energy spectrum using QGSJet01 and SIBYLL 2.1 simulations. The shaded band represents the estimated systematic uncertainties for the QGSJet solution, being of the same order as for the SIBYLL solution.

Figure 7 shows the two-dimensional correlation of measured (GeV) muon and electron sizes of showers. These data are unfolded and compared to simulations. The unfolding procedure compares the two-dimensional electron-muon numbers to simulations of air showers with primaries arranged into 5 elemental groups. Each group has its own energy spectra and cutoff energy. The analysis is based on a large number of simulations using two different high-energy hadronic interaction models, QGSJet and SIBYLL. On the right side of Figure 7 is the all-particle energy spectrum obtained from this procedure.

When separating the spectra for the five mass groupings, in either model the data require that the simulations give the lighter elemental groups their own knee features, which, when summed, is the main cause of the all-particle knee, as seen in Figure 8. There is notable model dependence in the result, especially for heavier primaries. The left side of Figure 8 shows the light and medium elemental abundances using QGSJet01 and SIBYLL. On the right, a striking difference is apparent for the heavier Si and Fe groups: SIBYLL gives a more “expected” result, with Si cutting off before the Fe group does.

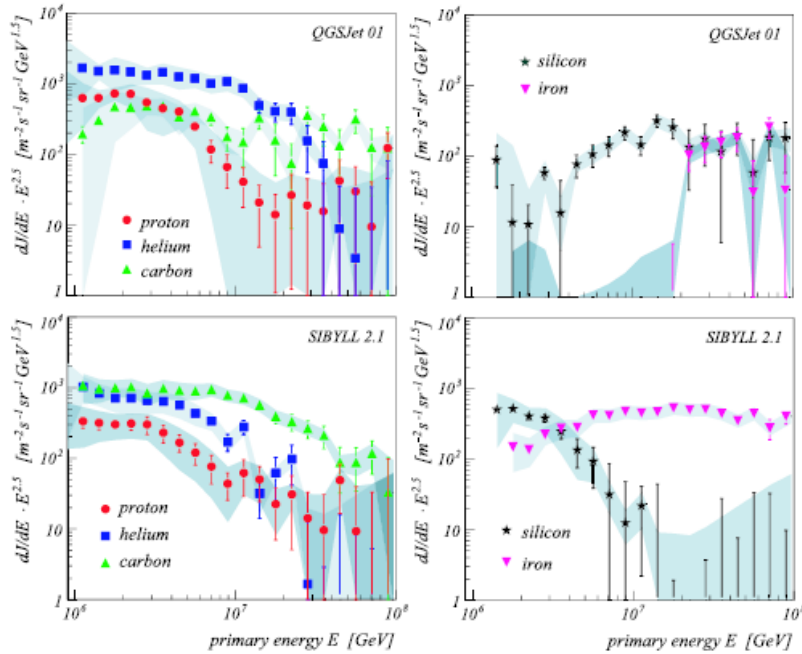


Figure 8: energy spectra for various elemental groups as measured by KASCADE, analyzed using QGSJet01 (top) and SIBYLL 2.1 (bottom) simulations. The shaded bands represent estimated systematic uncertainties.

The two simulations yield similar results for the all-particle spectrum, with the spectral knee at about 4 PeV. A new version of QGSJet – QGSJet02 – has also been employed and gives a result more similar to SIBYLL than to QGSJet01 (Figure 9). We will discuss the differences between the three interaction simulations in more detail in section 4 below.

When the correlated muon and electron sizes are examined in detail, the descriptions of the data by all three simulations show some problems and sensitivity to the characteristics of the interaction model used. Figure 10 exhibits the residuals of a χ^2 comparison of the data and the best-fit simulations. In the case of QGSJet01, at lower energies, the model predictions seem to be too light, since the distribution of muons cannot be well simulated over the range of observed sizes. On the other hand, QGSJet02 and SIBYLL both appear to need a heavier composition because the data has even more muons than can be accommodated by the best-fit fraction of iron at the higher energies.

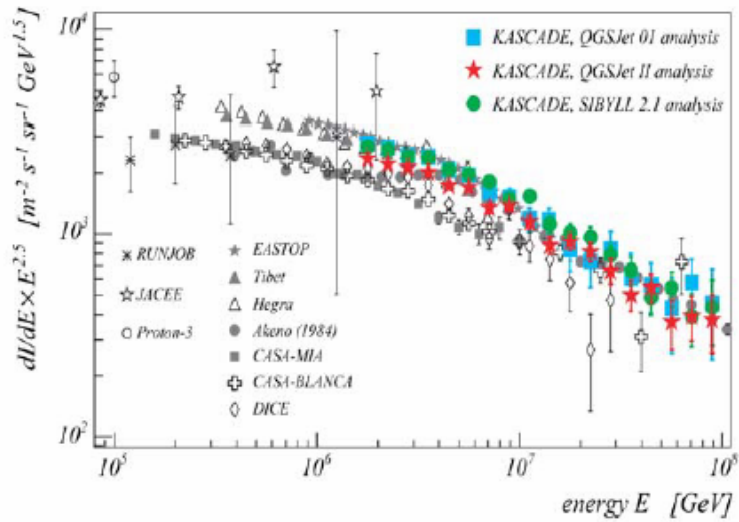


Figure 9: All-particle spectrum from KASCADE, using three interaction models.

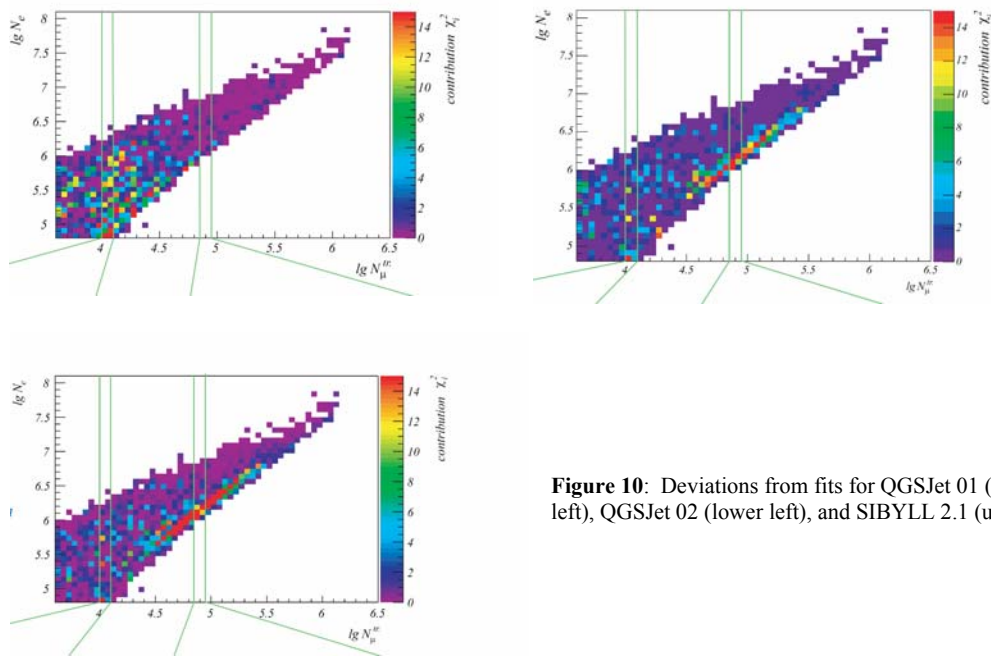


Figure 10: Deviations from fits for QGSJet 01 (upper left), QGSJet 02 (lower left), and SIBYLL 2.1 (upper right)

In summary, most experiments are yielding qualitatively similar results for the spectrum and for the composition of cosmic rays. A more exact determination of the spectrum and its components is limited now by the simulations.

4. Interaction Modeling

At the present time, the most often used high-energy interaction models for air shower simulation and data interpretation are QGSJet 01 [12] and Sibyll 2.1 [13]. At the conference a new version of QGSJet, called QGSJet 02, was presented. QGSJet 02 is theoretically more self-consistent than the old version and implements the results of the modern collider measurements. One of the most important changes was the introduction of modern parton density functions as measured at HERA[14], which predict a rapid growth of the number of gluons in a hadron with increasing energy. To obtain a consistent description of collider data up to Tevatron energy with these new parton densities, non-linear effects had to be introduced by summing so-called enhanced pomeron graphs[15]. The description of existing collider data and in particular also of fixed-target data in the 100 GeV range has been improved and a number of shortcomings of a technical nature of the old model version were addressed.

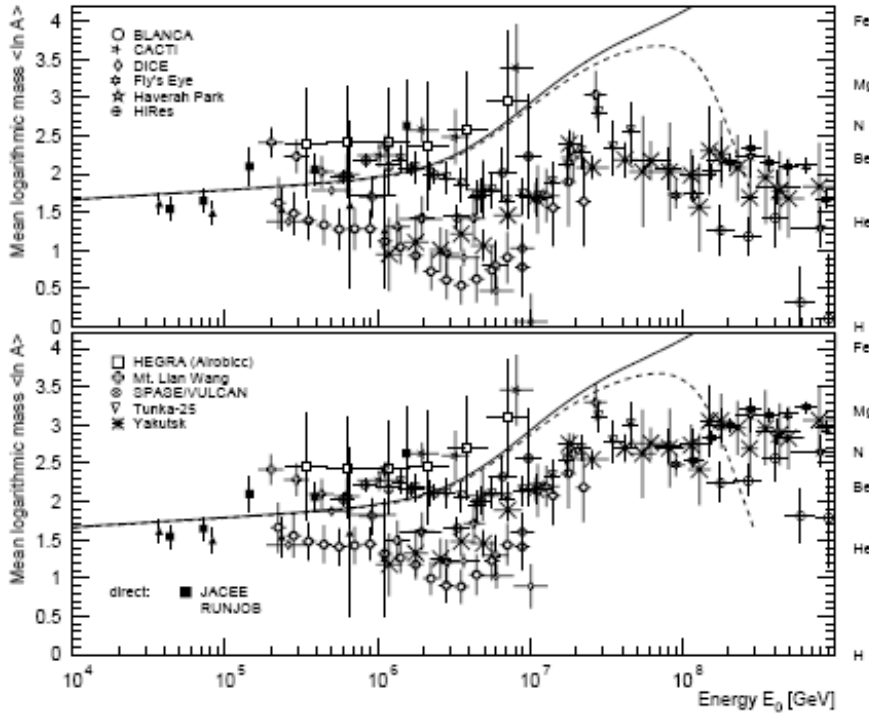


Figure 11: Mean logarithmic mass as inferred from measurements of depth of shower maximum, using two hadronic interaction models: the top shows results using QGSJET-I, while the bottom uses an early version of QGSJET-II [17]. The lines are predictions based on extrapolating direct measurements at lower energy with an exponential cut-off proportional to each element's Z.

The modification of the model implemented in QGSJet changes some of its predictions. In the following only a few are mentioned, a comprehensive comparison can be found in [16]. The proton-air cross section rises now faster than the prediction of QGSJet 01 but not as fast as that of Sibyll 2.1. The striking difference of the secondary particle multiplicity between QGSJet and Sibyll in p-air interactions is now significantly reduced at energies below 10^{17} eV. QGSJet 02 predicts a much lower multiplicity than the old version, only at the highest energies are the predictions almost the same. Also the elasticity (energy fraction of the leading hadron) is increased in QGSJet 02 in comparison to the previous version and is now very

similar to Sibyll. Concerning EAS, the new QGSJet version predicts a reduction of the muon number by 10-15%, an increase of the electron number and a shift of the depth of shower maximum deeper into the atmosphere by about 25 g/cm² for proton-induced showers. In general, the showers change to be more similar to that simulated with Sibyll, in particular, the mean depth of maximum is almost identical. Figure 11 illustrates the change in the interpretation of experimental data when different versions of QGSJET are employed [17].

The modification of the QGSJet predictions directly impacts the interpretation of EAS measurements. So far only the KASCADE Collaboration have re-analyzed their data using QGSJet 02. In contrast to the previous situation[18], the composition analysis of the KASCADE data with QGSJET 02 and Sibyll 2.1 leads to qualitatively very similar results[9]. Performing an analysis in terms of 5 elemental groups, the composition is dominated by He and C below the knee and turns heavier with increasing energy. It is interesting to note that, within the KASCADE energy range, indications for individual "knees" are found for all elemental groups but the heaviest group, Fe. However, neither the old or new version of QGSJet nor Sibyll give a perfect description of the high-statistics data sample of KASCADE, as we noted at the end of the previous section. Possible explanations are an underestimation of the number of muons and/or an overestimation of the electron number in showers initiated by heavy elements.

One of the very important tasks is the evaluation of the systematic error of the interpretation of EAS data due to the uncertainties of the hadronic interaction models. Some idea of the model dependence can be gained by using at least two interaction models for the necessary simulations. However, it is clear that the differences between, for example, QGSJet and Sibyll do not exhaust the full range of theoretical uncertainties. In particular, the decrease of the differences in the predictions of QGSJet 02 and Sibyll 2.1 does not mean that the uncertainties of the model extrapolations are significantly reduced now. First of all, there are uncertainties of each of the models which are related to its parameters[19,20]. Secondly, due to the lack of a calculable theory of the relevant interactions, there are theoretical uncertainties affecting mainly the high energy extrapolation [21].

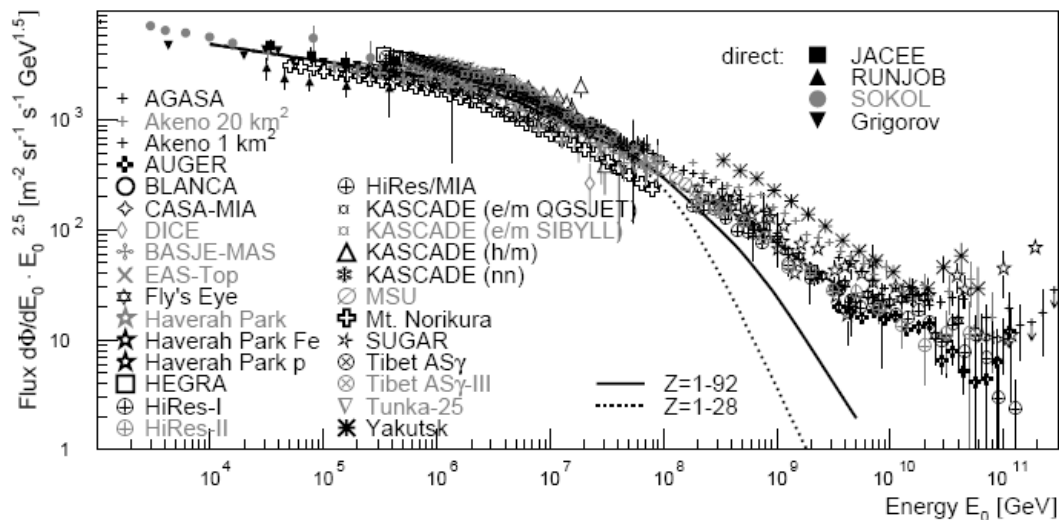


Figure 12. Compilation of all-particle energy spectra (from [17]).

5. Summary

It is instructive to examine all recent results on the cosmic-ray energy spectrum, including those from well above the knee and those well below it. Figure 12 gives these spectra, from a very recent review by Hoerandel [17] which includes most results from this conference. Taken together, it appears that there is a consistent picture of the *shape* of the spectrum, but there exist systematic *offsets* in energy scales between different experiments and, in some cases, different analyses of the same experiments. The overlaid lines in the figure are from a fit using the *poly-gonato* model [17], in which different primaries are assumed to have power-law spectra up to a point at which they undergo an exponential cutoff. Nevertheless, it is apparent that a reasonably consistent view of the spectrum is emerging, at least through the knee region, that is compatible with the “standard model” of Fermi acceleration in Galactic supernovae remnants.

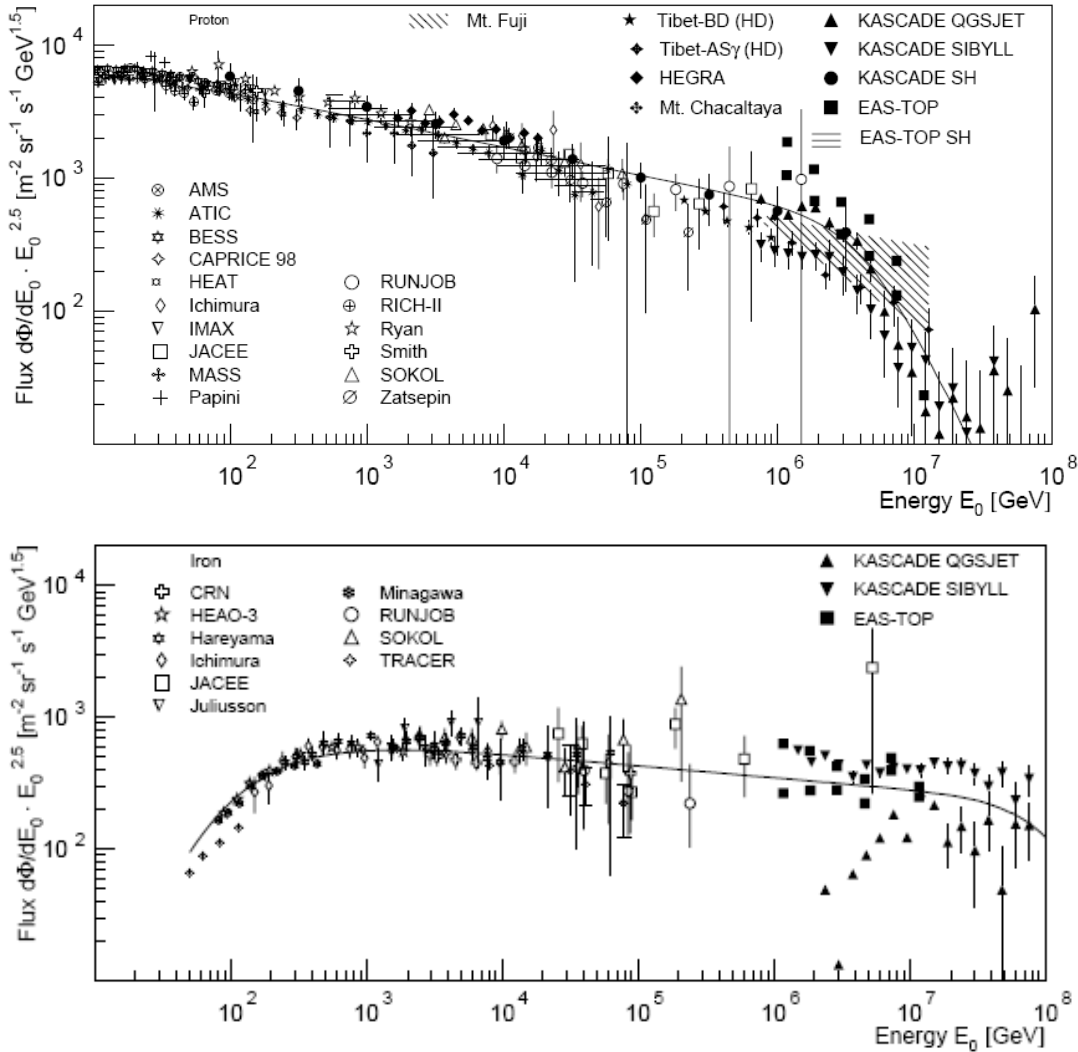


Figure 13. (Top) Proton energy spectra, including direct measurements at lower energy. (Bottom) Iron spectra.

The main difficulties in interpretations of the knee and how the composition varies through it are probably now seen in the interaction models. The differences between results is likely due, in large measure, to the particular simulation used. Figure 13 exhibits the Proton and Iron spectra from ground arrays ([17], and shown at this conference), compared to direct measurements at lower energy. The interaction model used is indicated, but note that “QGSJet” refers to QGSJet 01, not the newer version described in the previous section.

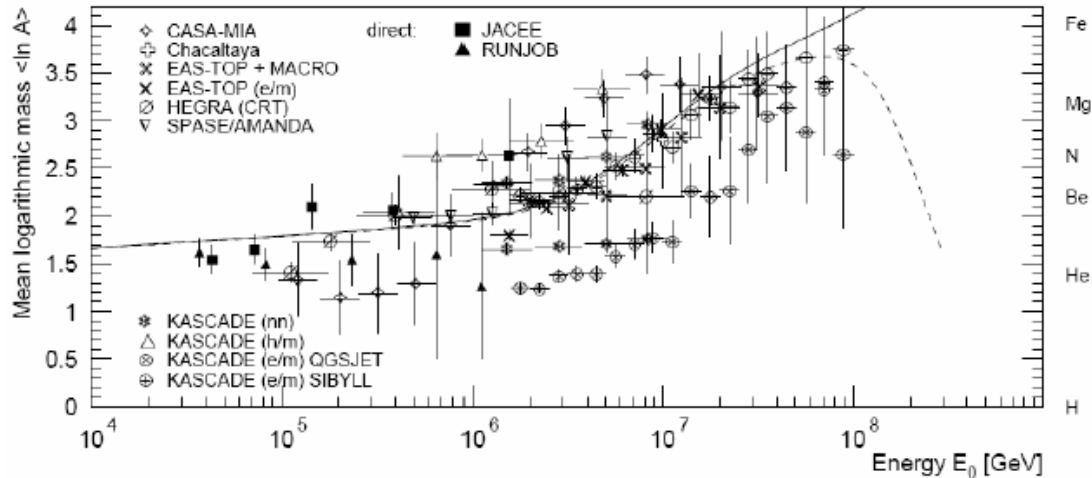


Figure 14: Mean logarithmic mass of cosmic rays derived from measurements of air shower particles at ground level.

The variation of mean logarithmic mass with energy is shown in Figures 14 and 15. Figure 14 compiles results from ground arrays, which have mainly used the correlated muon and electron sizes to infer the average primary mass. Figure 15 shows the same quantity from optical measurements of the depth of shower maximum. Note that the results in Figure 15 have been rescaled from their original publication using QGSJet02 [17].

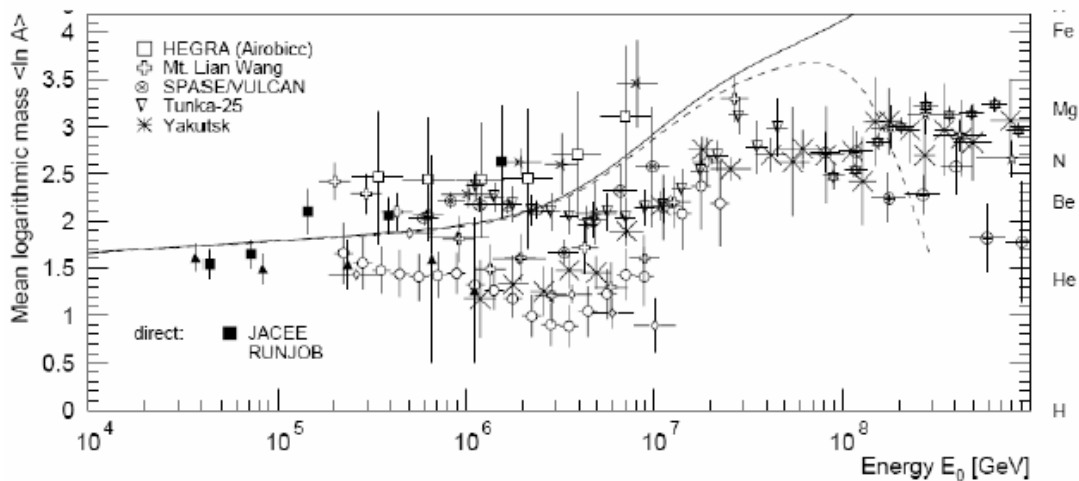


Figure 15: Mean logarithmic mass of cosmic rays derived from the depth of shower maximum measured by optical devices. These have been analyzed using QGSJET02 [17].

It is clear that using the new interaction modeling (either QGSJet02 or SIBYLL, which give very similar results), there is, perhaps for the first time, a strong consistency between the two approaches. Differences remain, but the trend toward higher mass primaries through the knee is seen in most experiments when analyzed using the same models. Those analyses which looked at spectra from individual or groupings of primaries mostly see evidence for individual knee features, appearing at larger energies for higher Z particles, as expected for SNR origins.

It is tempting now to wonder whether the differences at extreme energy between AGASA (a surface array) and HiRes (an optical device) can be reconciled using the improved simulations. These new interaction models give hope that a consistent picture is emerging. Jones and Martirosov have strongly advocated at this conference that a serious effort be undertaken to analyze different data sets with the same algorithms [22], the value of which is self-evident. But even though the main modeling schemes – QGSJet and Sibyll – have grown to give much more similar predictions, neither can fully explain all the details of the observed muon and electron production in air showers. While the models have made good use of available experimental data from accelerators, particle production at very small x , important for air showers, is difficult to obtain from collider experiments. Moreover, only when the LHC comes online will the interaction energy found in cosmic ray collisions near the knee become available for accelerator study.

6. Acknowledgements

The author thanks all the presenters in these sessions for their generous willingness to share their time and their talks with me, especially G. Navarra, A. Haungs, J. Hoerandel, and R. Engel. I am especially grateful to J. Hoerandel for his permission to use his recent summary plots and discussions with him on the overall experimental situation. I am also very thankful to the organizers of the ICRC, in particular Prof. S. Tonwar, who ran the conference well under very difficult circumstances, and who gave me extra time and understanding to complete this paper when I found myself in similarly difficult circumstances. This work was supported in part by the U.S. Department of Energy.

References

- [1] R. Ong, Rapporteur paper, Proc. 29th ICRC, Pune (2005), **10**, 329.
- [2] P. Bernardini, Proc. 29th ICRC, Pune (2005), **6**, 153.
- [3] M. Khakian Ghomi, Proc. 29th ICRC, Pune (2005), **6**, 29.
- [4] S.V. Ter-Antonian, Proc. 29th ICRC, Pune (2005), **6**, 101.
- [5] V.V. Prosin, Proc. 29th ICRC, Pune (2005), **6**, 257.
- [6] P.K. Mohanty, Proc. 29th ICRC, Pune (2005), **6**, 21.
- [7] G. Navarra, Proc. 29th ICRC, Pune (2005), **6**, 165.
- [8] M. Bertaina, Proc. 29th ICRC, Pune (2005), **6**, 41.
- [9] H. Ulrich, Proc. 29th ICRC, Pune (2005), **6**, 129.
- [10] A. Haungs, Proc. 29th ICRC, Pune (2005), **6**, 281.
- [11] H. Rebel, Proc. 29th ICRC, Pune (2005), **6**, 297.
- [12] N.N. Kalmykov, S. Ostapchenko, and A.I. Pavlov, Nucl. Phys. B (Proc. Suppl.) **B52**, 17(1997).
- [13] R. Engel, T.K. Gaisser, P. Lipari, and T. Stanev, T., Proc. 26th ICRC, Salt Lake City (1999), **1**, 415.
- [14] H. Abramowicz and A. Caldwell, Rev. Mod. Phys. **71**, 1275 (1999)
- [15] S. Ostapchenko, preprint hep-ph/0501093 (2005).
- [16] D. Heck, at VIHOS CORSIKA School 2005, Lauterbad, Germany <http://www-ik.fzk.de/~corsika/corsika-school/program.htm>

- [17] J. Hoerandel, “Workshop on Physics of the End of the Galactic Cosmic Ray Spectrum”, Aspen, 2005, preprint astro-ph/050814 (2005).
- [18] T. Antoni et al., *Astropart. Phys.* **24**, 1 (2005)
- [19] R. Engel, *Nucl. Phys. B (Proc. Suppl.)* **B122**, 40 (2003)
- [20] S. Ostapchenko, *J. Phys.* **G29**, 831 (2003).
- [21] H.J. Drescher, A. Dumitru, and M. Strikman, *Phys. Rev. Lett.* **94**, 231801 (2005).
- [22] L.W. Jones and R. Martirosov, *Proc. 29th ICRC, Pune (2005)*, **6**, 269.